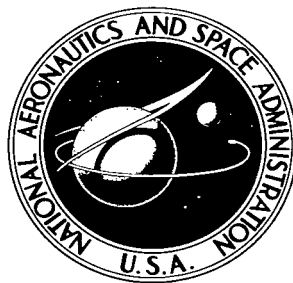


NASA TECHNICAL NOTE



NASA TN D-4220

c.1

LOAN COPY: RE  
AFWL  
KIRTLAND AFB, TX



TECH LIBRARY KAFB, NM

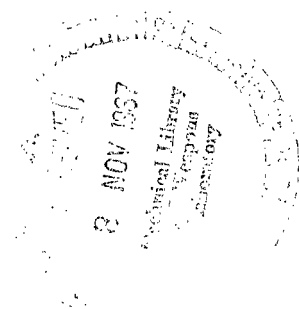
NASA TN D-4220

A COMPUTERIZED DATA-REDUCTION TECHNIQUE  
FOR LANGMUIR PROBE ANALYSIS OF  
ELECTRON TEMPERATURE VARIATIONS IN THE  
EXHAUST OF A MAGNETOPLASMA DYNAMIC ARC

*by David R. Brooks and James M. Hoell, Jr.*

*Langley Research Center*

*Langley Station, Hampton, Va.*





A COMPUTERIZED DATA-REDUCTION TECHNIQUE FOR  
LANGMUIR PROBE ANALYSIS OF ELECTRON TEMPERATURE VARIATIONS  
IN THE EXHAUST OF A MAGNETOPLASMA DYNAMIC ARC

By David R. Brooks and James M. Hoell, Jr.

Langley Research Center  
Langley Station, Hampton, Va.

NATIONAL AERONAUTICS AND SPACE ADMINISTRATION

---

For sale by the Clearinghouse for Federal Scientific and Technical Information  
Springfield, Virginia 22151 - CFSTI price \$3.00

A COMPUTERIZED DATA-REDUCTION TECHNIQUE FOR  
LANGMUIR PROBE ANALYSIS OF ELECTRON TEMPERATURE VARIATIONS  
IN THE EXHAUST OF A MAGNETOPLASMADYNAMIC ARC

By David R. Brooks and James M. Hoell, Jr.  
Langley Research Center

SUMMARY

A computerized technique is described whereby Langmuir probes may be used effectively to obtain detailed local measurements of electron temperature in the plasma beam produced by a 5- to 10-kW magnetoplasma dynamic accelerator. To achieve the necessary spatial resolution, on the order of 1000 values of electron temperature must be obtained for each operating condition of the accelerator. A 60-Hz probe-driving voltage and an automatic data-reduction system are used to obtain and analyze Langmuir probe characteristics. Accurate position correlation is provided by a specially designed probe driver. Probe curves and position information are recorded on FM tape and digitized for processing on the Langley IBM 7040-7094 DCS computer system.

Analytical problems encountered when interpreting Langmuir probe characteristics in high-power magnetized plasmas are discussed. A detailed description is given of methods for coping with large quantities of probe data which represent a wide spectrum of operating conditions. It is shown that, in the MPD arc, position surveys of electron temperature may be given as values averaged over scattered data with a standard deviation resulting from electron-temperature fluctuations in time.

INTRODUCTION

One of the basic problems encountered in magnetoplasma dynamic accelerator research is the detailed analysis of the structure of the plasma exhaust beam produced by such devices. The importance of this information cannot be overemphasized, for only through knowledge of local properties of the plasma beam can acceleration mechanisms be understood and optimized. As opposed to a previously published computer technique (ref. 1) suited for limited analysis of probe data obtained from relatively quiescent plasmas, the independently derived techniques described here are particularly suited for complete analysis of large quantities of data obtained in extensive surveys of the highly structured environment of the MPD arc.

The plasma produced by the MPD arc poses formidable diagnostic problems. Measurements are complicated by the existence of a three-dimensional structure in ion flow velocity with an axial flow velocity on the order of  $10^4$  meters/second, and a radial and axial structure in electron temperature, potential distribution, and density. In addition, the structural complexity makes difficult the use of some measurement techniques which would otherwise be desirable because they do not involve actual placement of a probing device in contact with the plasma. (The disadvantage of such methods is that they are generally best suited only for average measurements in fairly homogeneous plasmas.) Finally, when forced to use probing devices to uncover internal structure, the investigator is faced with the dual problem of (a) constructing and maintaining diagnostic equipment which will perform reliably both mechanically and electrically in a vacuum environment under the high heat loads presented by the plasma beam and (b) interpreting results obtained in an environment that is electrically noisy and structurally complex and that requires the variation of many independent parameters for a complete picture of arc behavior.

The plasma beam (having a charge density of about  $10^{11}/\text{cm}^3$  to  $10^{13}/\text{cm}^3$ ) is in principle accessible to analysis through the use of Langmuir probes. The analytical problems peculiar to free molecular Langmuir probe theory as applied to probes used in MPD arcs arise from the presence of a large ion flow velocity and an axially symmetric dc magnetic field with an intensity on the order of  $0.01 \text{ Wb/m}^2$  in the region of measurement. Once probe characteristics have been obtained under such conditions, there is a large body of work, both theoretical and experimental, to aid in their interpretation. (A comprehensive bibliography is found in ref. 2.)

In the idealized case of a quiet unmagnetized plasma, the information available from Langmuir probes includes electron temperature, plasma potential, and, indirectly, density and charged-particle flow velocities. However, the only plasma parameter that can be obtained directly from a probe characteristic taken in an MPD arc is the electron temperature. The other important parameters, including plasma potential, must be calculated in an indirect manner which in each case includes a theoretical dependence on electron temperature. Hence detailed knowledge of electron temperature is especially important to analysis of the MPD arc and, because of the relative ease with which other parameters can be included once the theory is known, the basic purpose of the probe data acquisition and reduction system is to provide a detailed survey of electron temperature. It is the purpose of this technical note to describe such a system, designed for use in conjunction with a high-speed digital computer.

## SYMBOLS

B	magnetic field, webers/meter <sup>2</sup> (Wb/m <sup>2</sup> )
C	thermionic emission constant, amperes/centimeter <sup>2</sup> /(degree Kelvin) <sup>2</sup> (A/cm <sup>2</sup> /°K <sup>2</sup> )
e	magnitude of electronic charge, coulombs (C)
I <sub>e</sub>	electron current, amperes (A)
j	current density, amperes/centimeter <sup>2</sup> (A/cm <sup>2</sup> )
k	Boltzmann constant, joules/degree Kelvin (J/°K)
m <sub>e</sub>	electron mass, kilograms (kg)
n <sub>e</sub>	electron density, number/meter <sup>3</sup> (number/m <sup>3</sup> )
r	radial position with respect to center line of plasma exhaust, centimeters (cm)
r <sub>L</sub>	Larmor radius for electrons, meters (m)
r <sub>p</sub>	probe radius, millimeters (mm)
T	probe temperature, degrees Kelvin (°K)
T <sub>e</sub>	electron temperature, degrees Kelvin (°K)
V	probe potential with respect to cathode of plasma accelerator, volts (V)
v	thermal velocity of electrons, meters/second (m/sec)
λ <sub>D</sub>	Debye distance, meters (m)
σ	standard deviation
φ	work function of probe, volts (V)

# APPARATUS

## Plasma Accelerator

The plasma accelerator used for the measurements described herein has a hollow cathode and porous anode (fig. 1). A wide range of mass-flow conditions can be obtained by separately adjusting the gas flow through the porous carbon anode and the center of the hollow tungsten cathode. The accelerator operates with argon at power levels from 5 to 10 kW, with magnetic field strengths from 0.07 to 0.20 Wb/m<sup>2</sup> (measured on the center line at the leading edge of the anode). The total gas-flow rate varies from 3 to 14 mg/sec.

The device is operated in a vacuum tank 1.7 m in diameter and 5.5 m long with an ambient pressure of  $0.5 \times 10^{-3}$  torr at the highest flow rates used (1 torr = 133.3 N/m<sup>2</sup>). To minimize wall interaction, the accelerator is electrically floated with respect to the grounded tank and is situated approximately on the center line of the tank. Parametric studies with an accelerator having a hollow cathode and porous anode have been previously reported by Weinstein and Hoell (ref. 3).

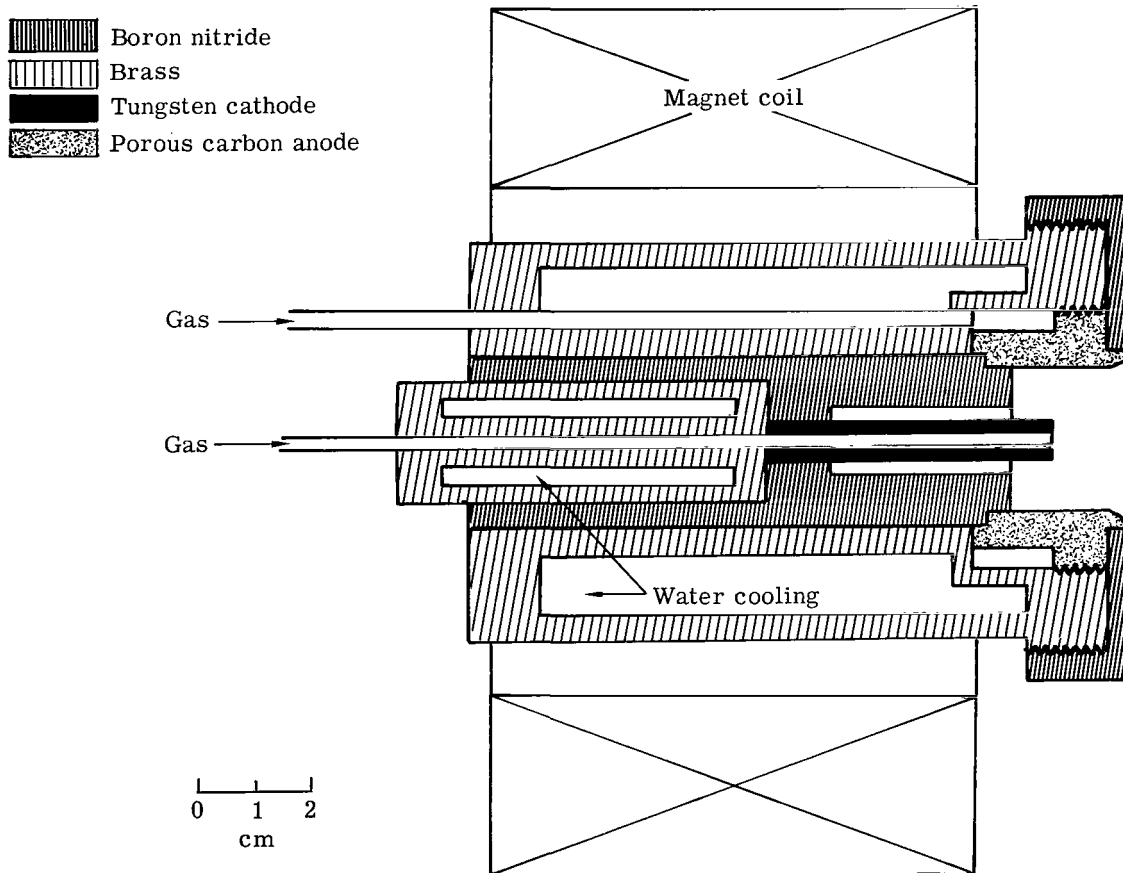


Figure 1.- Arc jet with hollow cathode and porous anode.

## Probe-Driving Mechanism

Since the exit diameter of the plasma beam is 2.5 cm, spatial resolution must be on the order of millimeters if meaningful data are to be obtained concerning the structure of the beam. To satisfy the need for position-correlated data, a probe-driving mechanism has been constructed (fig. 2). It operates smoothly even at the base pressure of the vacuum system used for these measurements ( $\approx 10^{-5}$  torr). Alternating-current motors with dc braking provide three independent drives, giving three degrees of freedom in a stan-

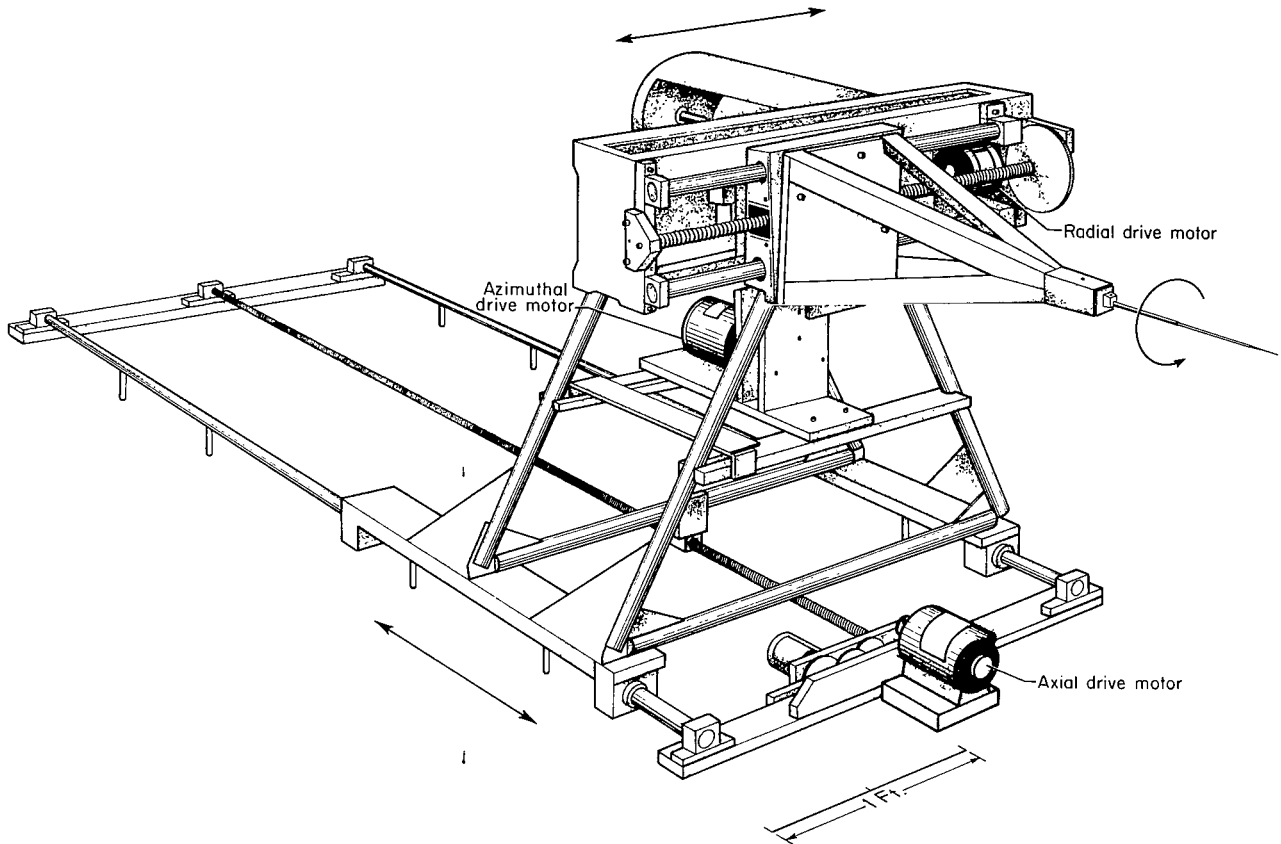


Figure 2.- Motorized probe-driving assembly giving three degrees of freedom.

dard cylindrical coordinate system. Driving speed is about 2 cm/sec. Position output signals are provided by precision 10-turn potentiometers, and an absolute accuracy of better than  $\pm 1$  mm is possible. To minimize electrical interference with the discharge, the aluminum boom that holds the probe is electrically isolated from the rest of the driver.

## Data-Acquisition System

The probe circuit, with associated recording equipment, is shown schematically in figure 3. Line voltage is isolated and continuously variable through a step-up

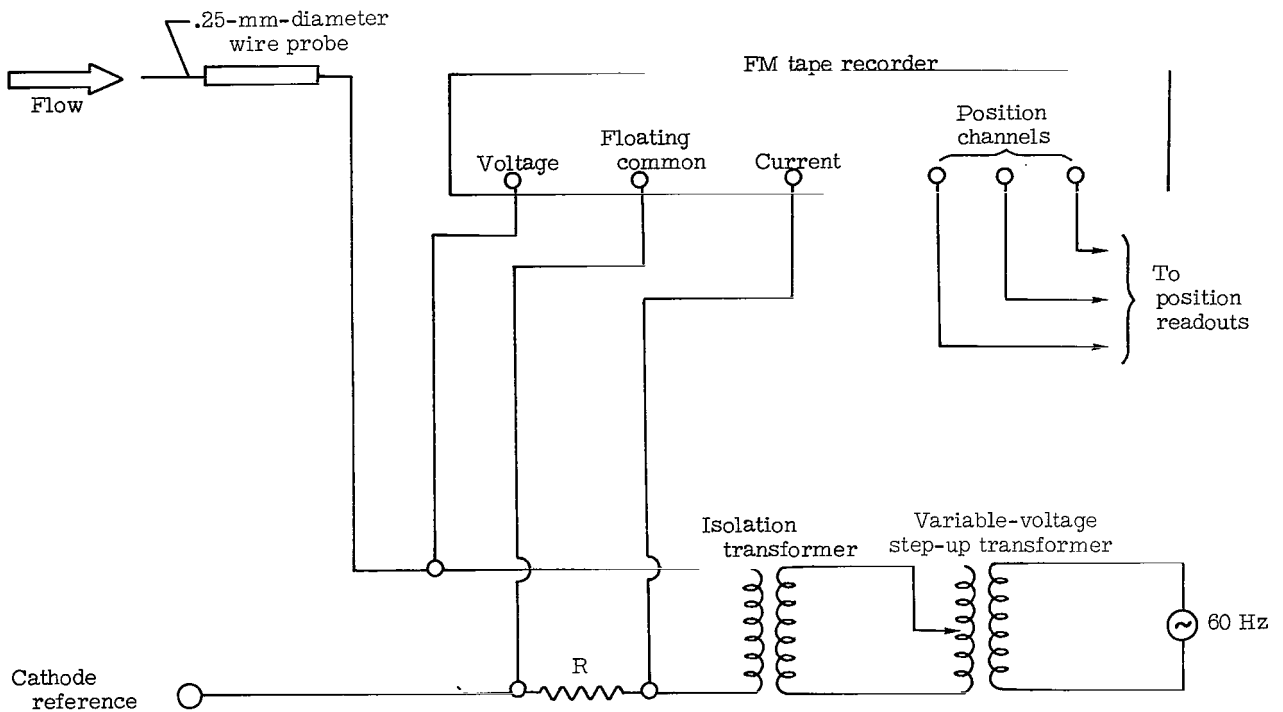


Figure 3.- Probe circuit and recording equipment.

transformer. Probe current, voltage, and as many as three position channels are recorded on an FM tape recorder. The resistor  $R$  serves both as a current limiter and as the source of the current signal. The probe itself is constructed of 0.254-mm-diameter iridium wire (chosen because of its low thermionic emission) and high-density alumina tubing. It is aligned parallel to the flow axis with 7.65 mm of bare wire exposed to the flow.

An essential feature of the data-acquisition system is the ability to achieve the necessary spatial resolution by providing a large number of probe curves while the probe is actually moving continuously through the discharge. The 60-Hz sweep rate provided by line voltage is well suited to surveys with the existing drive speeds. It provides a reasonably short elapsed time between curves so that details of very low-frequency time fluctuations can be retained rather than averaged out. With a driving speed of 2 cm/sec, the maximum spatial resolution is 48 curves per centimeter. During the time required for each probe curve (8 msec), the probe moves about 0.16 mm, which is less than the available absolute spatial resolution.

The full bandwidth of standard FM tape recorders (0 to 20 kHz) is desirable for recording and initial playback of data in its analog form. For conversion into digital form, however, data that are too noisy for efficient reduction can be low-pass filtered electronically on playback. This method has a decided advantage over including filtering



in the probe circuit because the degree of filtering can be more readily adjusted to particular situations during the data reduction process. For the present system, a 1760-Hz (real time) low-pass filter is used in all cases. This value is about 250 Hz higher than the minimum upper cutoff frequency that can be used without distorting the essential shape of the probe curves. (The filter must pass much more than the 60-Hz sweep frequency because the exponential nature of the probe current-voltage curve gives a relatively fast rise time to part of the current and voltage signals.)

## LANGMUIR PROBE DATA REDUCTION

### Analysis of Probe Curves in High-Power Magnetized Plasmas

The basic collisionless Langmuir probe theory is well known (ref. 2). For purposes of definition, the procedure for obtaining the electron temperature  $T_e$  will be briefly summarized. From the probe current-voltage characteristic (I-V plot), electron current is computed by subtracting an extrapolation of the ion saturation current from the net probe current. Then, for Maxwellian electrons in the retarding field of the probe, the electron current density at the probe surface is given by

$$j_e = j_{e,0} \exp(eV_{pl}/kT_e)$$

where  $j_{e,0}$  is the random electron current density in the undisturbed plasma and  $V_{pl}$  is probe voltage with respect to the plasma. Taking the logarithm of both sides shows that for a Maxwellian distribution, the logarithm of the electron current is a linear function of probe voltage. The electron temperature can be found by differentiation:

$$\frac{e}{kT_e} = \frac{d(\ln j_e)}{dV_{pl}} = \frac{d(\ln I_e)}{dV}$$

That is, the slope of the curve of  $\ln I_e$  as a function of  $V$  is inversely proportional to  $T_e$ . It is important to bear in mind that a temperature is defined in the usual sense only for the case where  $d(\ln I_e)/dV$  is actually a straight line.

For Langmuir probe diagnostics in MPD arcs, only a limited portion of the theoretical probe curve is available for analysis under experimental conditions of interest. There are two basic reasons for this limitation: (1) the presence of a dc magnetic field which distorts the electron saturation end of the probe curve and (2) thermal problems caused by the excessive electron current which can be drawn from a high-current device.

At present there is no general theory which relates plasma parameters to Langmuir probe curves taken in the presence of an imposed magnetic field. While a detailed discussion of the problem is beyond the scope of this technical note, it is important to

understand the possible effect of a magnetic field on Langmuir probe measurements. Whereas for geometrically symmetric Langmuir probes, electron collection in an unmagnetized plasma is isotropic and localized within roughly a few Debye distances from the probes ( $\lambda_D \approx 69\sqrt{T_e/n_e}$  meters), a large external magnetic field results in highly anisotropic and nonlocalized collection when  $r_L < r_p$ , where  $r_L$  is the electron Larmor radius,  $vm_e/eB$ . Because of the relative ease with which charged particles move along magnetic-field lines, all probes would become, roughly speaking, plane probes which see a particle flux streaming along a tube of radius  $r_L$  and undetermined length  $l$  parallel to the flux lines.

Since  $l$  can be much greater than the Debye length, the probe can collect a large part of its current from some other location many Debye distances away and the local nature of the measurement would be destroyed. However, even with a magnetic field it is possible to define portions of the probe curve, depending on particle energies and field values, where the Larmor radius for the collected particles is still larger than both the Debye length and the probe diameter. For the accelerator described herein, typical values, within an order of magnitude, are  $\lambda_D \approx 0.01$  mm,  $r_p \approx 0.1$  mm, and  $r_L \approx 1$  mm. Larmor radii of ions are at least 100 mm. Under such conditions, the probe theories for localized collection in unmagnetized plasmas (zero-field approximation) should apply. Clearly, if such regions exist, they will correspond to the regions where ions (large mass) or high-energy electrons (large velocity) are collected. With respect to the voltage applied to the probe, these considerations mean that only the electron current corresponding to probe voltages near the floating potential can be used.

When interpreting probe curves obtained in a plasma accelerator, it is necessary to consider the possibility that electron temperatures may be a function of the orientation of the probe with respect to the magnetic field and the ion flow velocity. However, it has been shown that the magnetic-field orientation is not critical in the cases where the zero-field approximation may be applied (ref. 4) and that  $T_e$  measurements are not affected by the presence of a plasma flow velocity as long as the electron thermal velocity is much greater than the plasma flow velocity (ref. 5).

Another important problem of interpretation arises from the fact that Langmuir probe theories are generally predicated on Maxwellian electron distributions. One can question the accuracy of inferring a Maxwellian distribution from a high-energy tail that appears Maxwellian. This question cannot be answered directly without an independent determination of the complete distribution function. However, it is assumed that the entire distribution function is Maxwellian if the variation of  $\ln I_e$  with  $V$  is linear over the range of electrons being collected (about 10 percent of the total number for the measurements used in this work).

The electron current that can be collected by a probe in an MPD arc is always much larger than can be used practically. Unless the current level in the probe circuit is externally limited, enough electron current will be drawn to heat the probe to emission temperature and perhaps destroy it. In addition, the current may be an appreciable fraction of the total arc current, in which case the effectiveness of the probe as a diagnostic tool is destroyed. Fortunately, the lower electron-current level that is compatible with these considerations merely eliminates the portion of the probe curve that cannot be used in the presence of a magnetic field.

During normal operation the probe used for these measurements is hot enough to emit visible light but is still below the temperature at which electron emission becomes a serious problem. For example, at the highest arc powers tested the probe reaches a temperature of  $2100^{\circ}$  K at a distance of 5.0 cm downstream from the anode face when left exposed to the flow for several seconds. The temperature reading, made with a micro-optical pyrometer, is only approximate since the emissivity of the iridium wire is not precisely known. However, the Dushman equation,  $j = CT^2e^{-e\phi/kT}$ , can be used to provide an upper limit on emission for a particular temperature. For the iridium probe used, taking  $C = 100 \text{ A/cm}^2/\text{K}^2$ ,  $\phi = 5.31 \text{ V}$ , and a probe area of  $6 \times 10^{-2} \text{ cm}^2$ , an emission current of less than  $10^{-5} \text{ A}$  is predicted at  $T = 2100^{\circ} \text{ K}$ . This value is negligible with respect to the probe current levels encountered ( $\approx 10$  to  $100 \text{ mA}$ ). If the probe is moved too close to the accelerator electrodes, typically closer than 2 anode diameters, substantial thermionic emission occurs even when probe exposure time is minimized. This effect provides the limit on the distance of closest approach to the electrodes.

#### Reduction of Taped Data

The use of tape recording and its associated computerized processing is admittedly an indirect and complex process, but it is necessitated by the following fact: to achieve the required spatial resolution both axially and radially, approximately 1000 probe curves must be analyzed for each running condition. In the case of the hollow-cathode accelerator, a running condition is specified by four independent quantities: cathode and anode gas flow, arc current, and magnetic field.

It is estimated that in the course of developing the computer techniques described in this technical note, at least 20 000 separate probe curves have been processed. With this quantity of data, it is obvious that (1) data reduction cannot be efficiently accomplished by hand, and (2) to achieve much increase in efficiency, the time required to set up a computerized data-reduction system and guide a large flow of information through several stages of processing must be compensated for by a resulting system that does not require numerous programming changes to handle the unavoidable changes in the detailed behavior of the data. In order to develop an efficient reduction system, several steps were decided upon at the initiation of the experimental program:

(1) FM recordings were to be the only storage facility for the data. This method is convenient for computer input and also permanently preserves the data in its original analog form for playback through an x-y oscilloscope or other analog readout device.

(2) The computing procedures were to include criteria in the program for distinguishing between the end of one curve and the beginning of the next. Thus a data tape containing several hundred curves could be automatically processed from start to finish without the manual addition of timing markers or counting of points.

(3) The inevitable problem of noise in the probe data was to be handled not by manually rejecting particularly noisy curves or bad points (which would involve a prohibitive amount of time) but by careful choice of computing techniques and a simple method of analyzing the success of each computing step. Computer plotting routines with 35-mm film output have provided the solution.

The reduction of analog FM tapes is accomplished as shown schematically in figure 4. (The Fortran IV program written for this project is available from the authors.) The data tapes are converted from analog to digital form by the Langley Adtran (analog to digital transcriber) system. The necessary time resolution is provided by recording at a tape speed of 60 in./sec (152.4 cm/sec) and playing back at  $3\frac{3}{4}$  in./sec (9.5 cm/sec). The present data-reduction setup provides 1850 points per second at the playback speed. Thus, the real-time resolution is  $16 \times 1850$ , or 29 600 points per second. As a probe curve is recorded in 8 msec, there is a resolution of about 240 points per curve. This high degree of resolution, required for noisy data, is evident in curve 1 of figure 5, which shows a sample computer-generated plot of

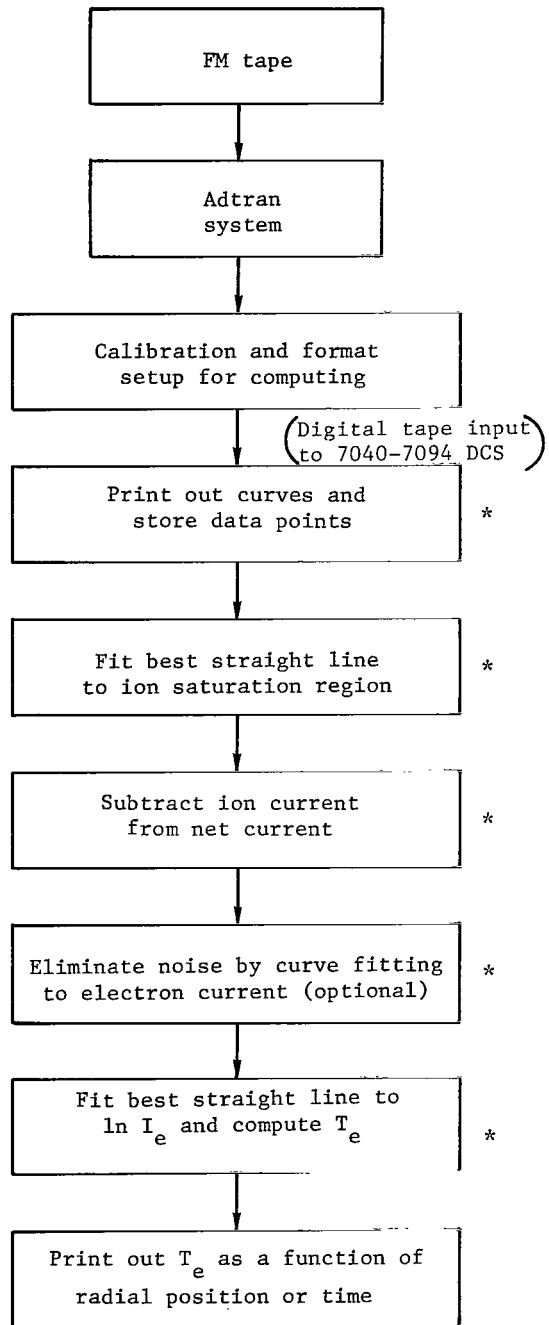


Figure 4.- Block diagram of data-reduction procedure. Asterisk (\*) denotes visual inspection on 35-mm film.

a typical probe curve. (This figure is explained in detail subsequently.) The signal resolution of the digitizer is  $\pm 900$  units for  $\pm 100$ -percent modulation. Based on a standard tape input sensitivity of 1 V rms for 100-percent modulation, the signal resolution is typically  $100 \mu\text{A}$  for 200 mA peak-to-peak probe current and 100 mV for 200 V peak-to-peak probe voltage.

A block diagram of the Adtran control system developed for this project and corresponding voltage outputs from the numbered points are shown in figures 6(a) and 6(b), respectively. With the circuit of figure 6(a) it is possible to digitize a preselected fraction of the total number of curves by using a binary counter. The digitizing process is controlled by two Schmitt triggers, one of which has as its input the probe current channel, and one of which provides a sampling rate pulse generated by an audio-oscillator. The  $1/4$ -cycle delay locates the ion saturation region (most negative current), and the pulses generated are counted. When the appropriate number has been reached (2 in this case) the  $1/2$ -cycle delay unit is triggered to provide the necessary signal to the AND gate for starting and stopping data digitization at the rate established by the oscillator. Of course, for maximum spatial resolution, every curve can be digitized. But since a relatively

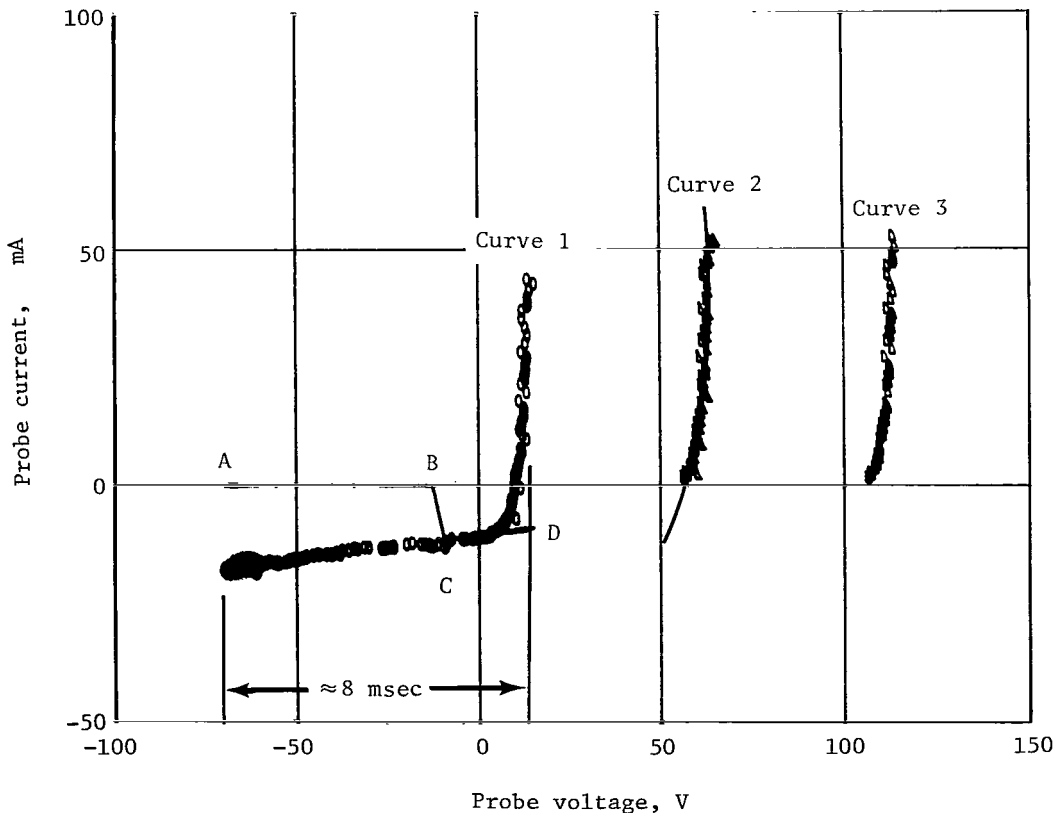


Figure 5.- Computer plot of typical Langmuir probe data and extraction of electron current.

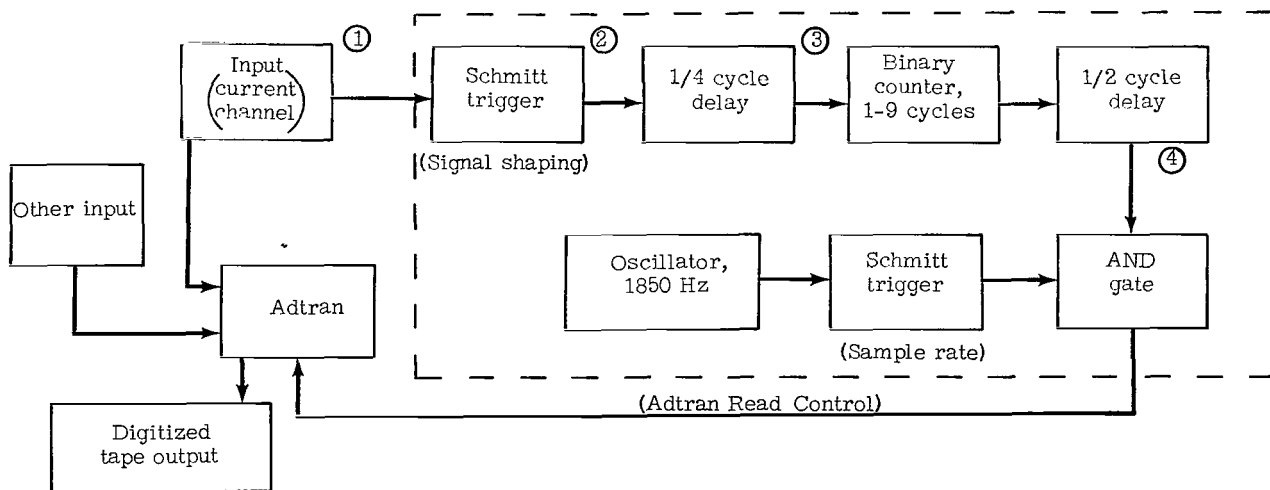
large amount of computer time is required for analysis of the data (an average value is 2 sec of IBM 7040-7094 computer time per curve), this system prevents the accumulation of more data than are required for a particular condition. It would be expected, for example, that spatial variations in the plasma beam would become less intense farther downstream because of beam spreading, diffusion, and recombination, and hence that fewer temperature points would be required to determine the structure of the beam.

The digitized tape from the Adtran is next reprocessed with predetermined calibration constants, and the result is a digital tape containing data in engineering units in a format suitable for retrieval during the actual computing process.

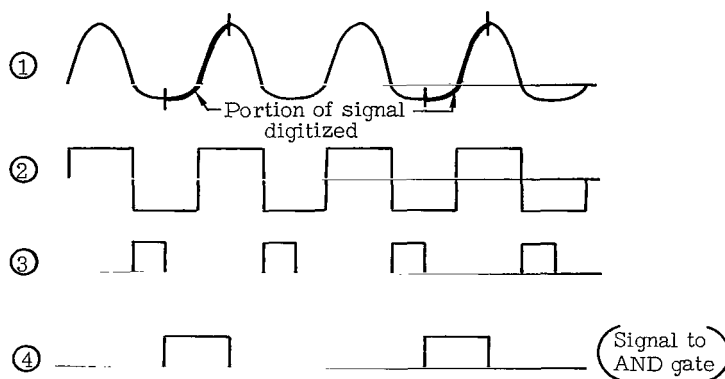
An important feature of the data reduction and analysis program written for the Langley IBM 7040-7094 DCS computer is the inclusion of computer-generated plots of the initial data and the results of all computing procedures. These plots are filmed for a permanent record and allow visual checks for each step of analysis. An example is shown in figure 5. Curve 1 is a plot of the original data points (I-V plot). The negative current corresponds to ion current. The abrupt cutoff of the electron current shows the effect of current-limiting in the probe circuit. The line ABCD is the result of a least-squares straight-line fit to the ion-current points over the voltage range AB. The number of points included in this fit is specified as a program input quantity. CD is an extrapolation of the line fitted to the ion current into the region where electron current is being collected. Visual examination of the line segment CD is mandatory to assure that it actually represents the slope of the ion current, since a particularly noisy curve occasionally produces a bad fit. More will be said concerning the fit to the ion current at the end of this section.

Calculation of  $T_e$  is accomplished as indicated previously. A set of electron-current points is generated by subtracting a value on the line CD from the corresponding point in the net current array. After several intermediate steps the logarithm of  $I_e$  is plotted as a function of voltage. If the electron distribution is Maxwellian, the variation of  $\ln I_e$  with  $V$  will be a straight line, and its slope determines  $T_e$ .

The data points that comprise the electron-current array are plotted in curve 2 of figure 5. To avoid taking the logarithm of small numbers as the electron current goes to zero, data points corresponding to less than 2 mA are discarded. The solid line along the data points of curve 2 represents a second-order polynomial fit to the electron-current array. At this point, the effects of random noise can be reduced by eliminating data points whose residual exceeds by a specified amount (in magnitude) the standard deviation  $\sigma$  computed for each curve fit. In this case,  $2\sigma$  has been used as an arbitrary cutoff criterion, with results as shown in curve 3 of figure 5, which contains the electron-current array minus the points discarded by residual testing. (Four points have been discarded



(a) Adtran control block diagram.



(b) Voltage waveform at numbered points.

Figure 6.- Block diagram for control of data digitization (set for every second cycle).

in this figure.) The inclusion of a polynomial fit to the electron current for the purpose of noise reduction is, of course, optional and need not be included if the data are clean.

Figure 7 shows a plot of the final stage of computing. In this figure, the points represent the logarithm of the electron current and the solid line represents the straight-line fit to these points. The increase in point density for higher current does not represent, as it might seem, an increase in the noise level, but is due to the current saturation imposed by the probe circuit. The time interval between digitized points is constant, so as the current tends to saturate, the difference between one point and the next becomes smaller. It is the slope of this solid line which determines  $T_e$ , given as printed output along with corresponding position or time. It is clearly essential to inspect such a figure for each probe curve. The computer program will produce a "temperature" for an

arbitrary collection of points, but the result is meaningful only when the logarithm of the electron current is in fact a straight line. The criteria for acceptability of a particular result will be discussed in the next section. An example of the results achieved is shown in figure 8, which is representative of the computer treatment of probe curves obtained in the hollow-cathode device. This figure is a composite of several computer-generated

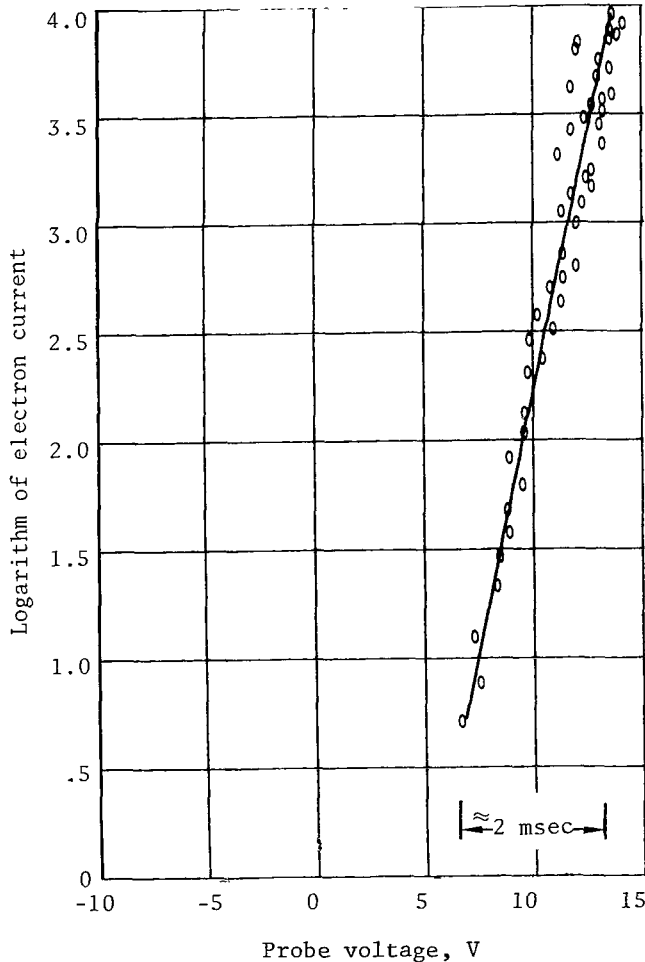


Figure 7.- Computer plot of  $\ln I_e$ -V and straight-line fit for determining  $T_e$ .

temperature curves for various radial positions. The shift along the voltage scale is due to the radial variation in floating potential.

A  $\ln I_e$ -V plot which does not yield a straight line can, of course, be questioned on the grounds that it does not represent a Maxwellian electron distribution or that arc conditions have changed during the recording of the curve, but it can also be questioned on the grounds that the fit to the ion current may not be reasonable. To assure the best possible ion-current fit, the I-V plot is divided into two parts corresponding to the broken line ABCD in figure 5, as previously explained. The number of points used to obtain the fit to the ion saturation current (line AB) is specified as an input value to the computer program, first by estimating the proper number of points based on past experience and later on the basis of resultant I-V plots. This number is constant for a particular operating condition, but is a strong function of each of the independently adjustable arc parameters as well as the probe sweeping

voltage and position. As a rule, a test run of a small number of curves is made for each running condition to adjust the length of line AB. After final processing the fits to the ion saturation current are as good as can be obtained, considering the slight uncertainty due to small fluctuations in the ion current, and it can be said with confidence that  $\ln I_e$ -V plots which are not straight lines are due to changing plasma conditions or non-Maxwellian distributions and not to the quality of the fit to the ion current.



Radial distance  
from center  
line, cm

0.104

0.643

2.032

3.221

6.198

$T_e, ^\circ\text{K}$

22 100

27 700

28 500

34 100

21 500

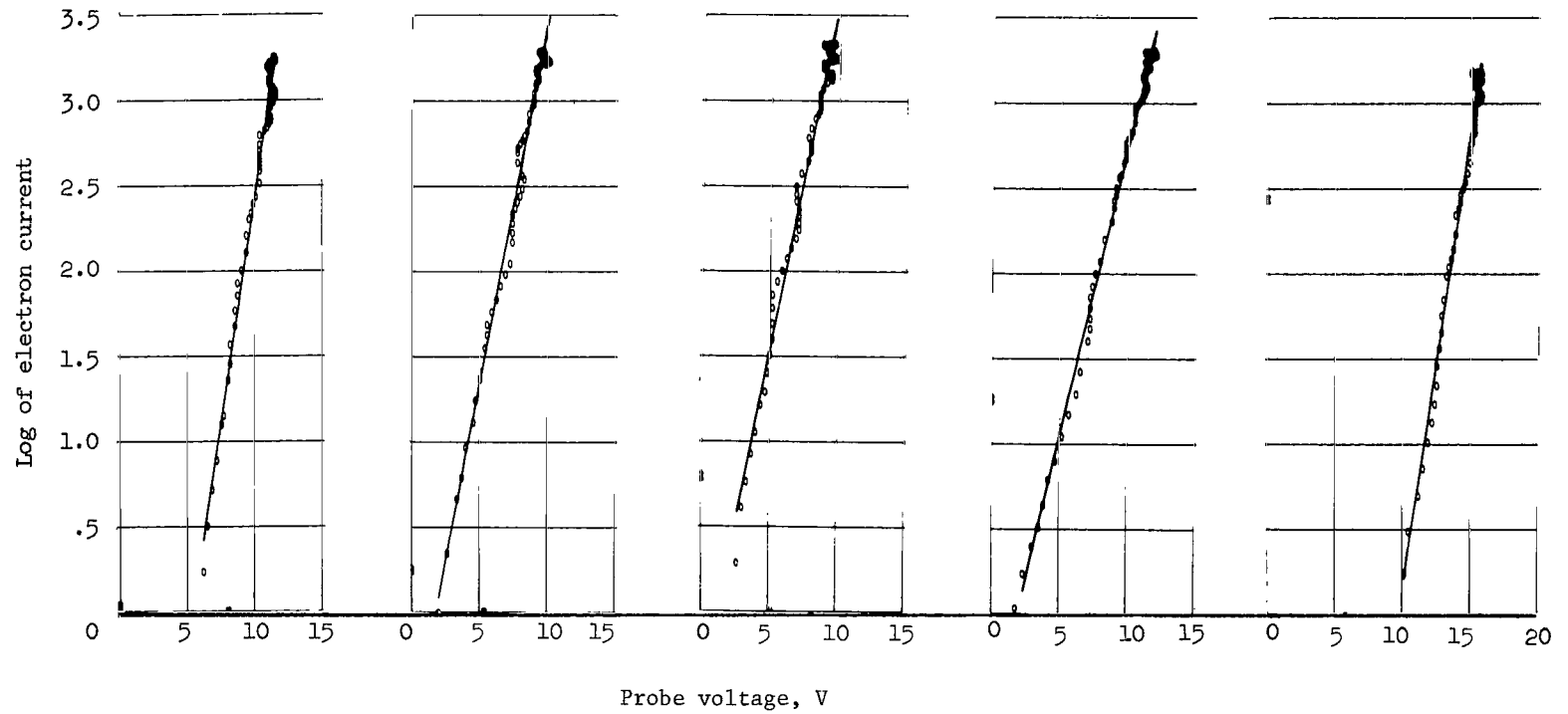


Figure 8.- Composite of several computer-generated  $T_e$  plots at various radial positions.

An additional note is in order concerning the method of determining the fit to the ion saturation current. When there is very little fluctuation in the ion current, as in figure 5, there are alternatives to fitting a straight line to a manually preselected number of points. For example, a minimum number could be chosen for a straight-line fit and points could be added by testing the residual of each point with respect to the straight-line fit established by all the preceding points. The advantage of this method is obvious – for smooth data the correct number of points is chosen automatically. However, this method is not reliable when noisy curves must be treated, since one wild point in the ion current may result in too few points being fitted and thereby cause an error in the extrapolated ion current.

### Interpretation of Experimental Results

When computed electron temperatures are plotted as a function of radial position across the central portion of the arc exhaust, as in figure 9(a), it is evident that considerable scatter exists in the results. (The  $T_e$  values plotted here are for different operating conditions than the  $\ln I_e$ - $V$  plots of fig. 8.) Examination of similar figures for a wide range of operating conditions has led to several conclusions concerning the scatter in  $T_e$  values:

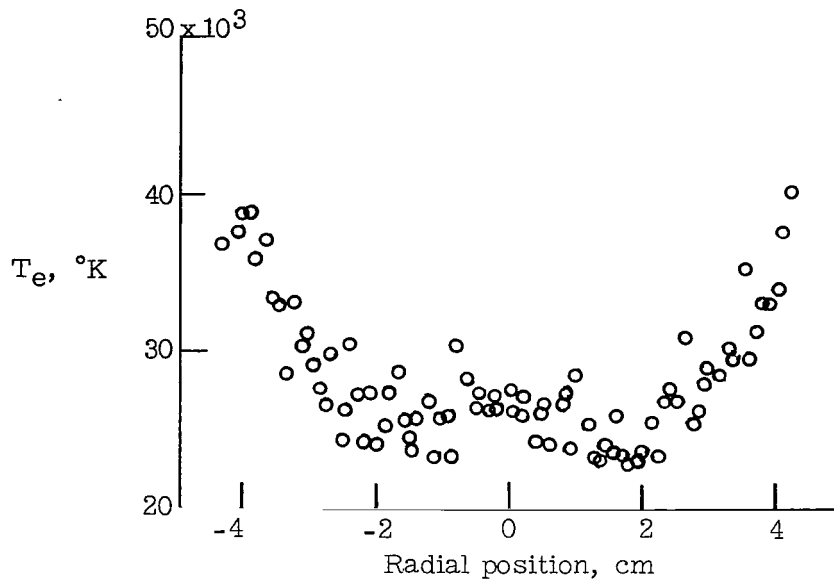
(1) Once an accurate fit has been made to the ion saturation current and once  $T_e$  has been defined as being inversely proportional to the slope of the best straight-line fit through the  $\ln I_e$ - $V$  data points, the computational error (resulting from, for example, a slight error in the slope of the line fitted through the  $\ln I_e$ - $V$  plot) is small compared with the actual differences in  $T_e$  which exist in the arc.

(2) The variations observed in figure 9(a) represent real  $T_e$  differences arising from both spatial and time variations in the arc exhaust.

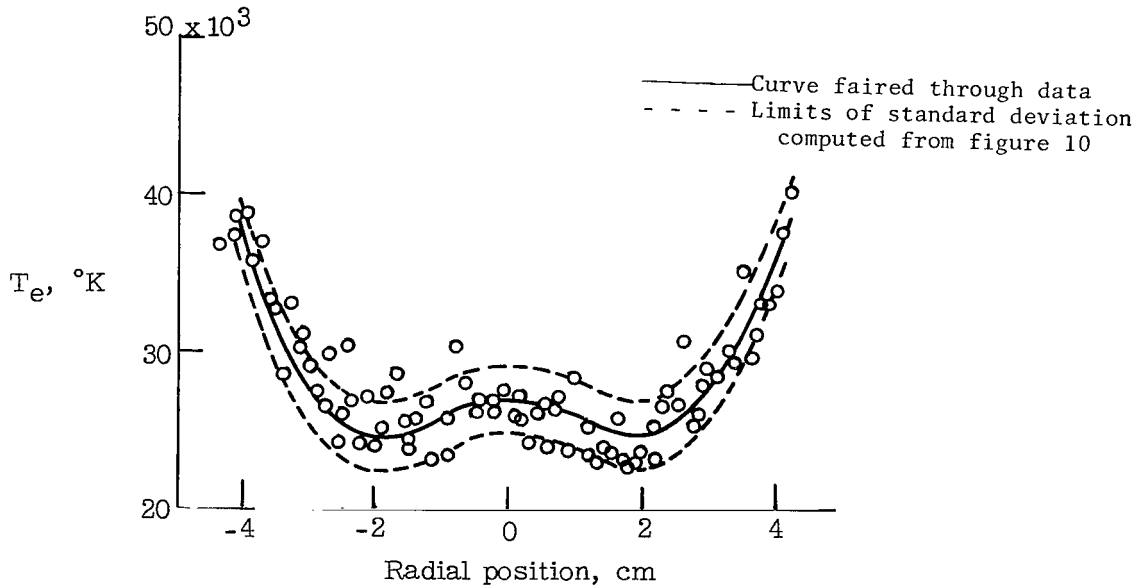
(3) It has been found that the peak-to-peak time fluctuations in  $T_e$  at a particular point in space are under some conditions as large as the apparent spatial variations in values of  $T_e$  across the radius of the exhaust.

(4) Because the nature of the MPD arc is such that it is necessary to make probe measurements in a relatively short period of time to avoid overheating, spatial surveys made with the moving probe described in this technical note always contain some ambiguity whenever time fluctuations in local plasma conditions have a component too slow to be averaged in the course of one measurement.

In an attempt to clarify the meaning of spatial surveys, which on the basis of the above conclusions are assumed to include both spatial and time variations in  $T_e$ , electron temperature distributions have been determined solely as a function of time at several fixed positions. Such a distribution is shown in figure 10, corresponding to the operating condition of figure 9(a). To obtain figure 10, the probe was placed at  $r = 0$  and probe



(a) Electron temperature as a function of radial position.



(b) Curve fit to data including computed standard deviation. Estimated mean temperature at  $r = 0$  is  $27\ 000^{\circ}\text{K}$ .

Figure 9.- Electron temperature as a function of radial position at an axial distance of 12 cm downstream from anode face.

curves were continuously recorded for a real time of about 5 seconds. The axial position, identical for figures 9(a) and 10, was far enough downstream so that the probe did not heat to emission temperature during the 5-second period. On the basis of such measurements it has been found that  $T_e$  varies randomly at a relatively low frequency in such a way that the temperature is generally constant during the time required for a measurement, typically 8 msec, but is generally different during the next measurement, which begins

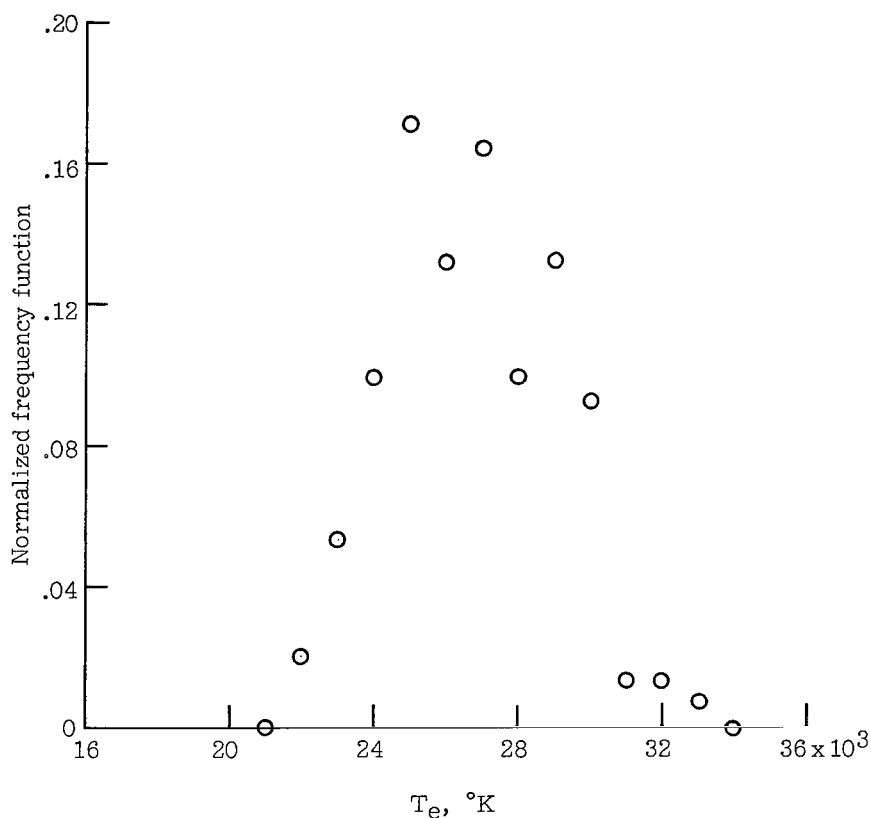


Figure 10.- Electron temperature distribution for the conditions of figure 9 at  $r = 0$ .  
 Sample time, 5 sec; number of samples, 152; mean temperature,  $26\ 500^\circ\text{K}$ ;  
 standard deviation,  $2300^\circ\text{K}$ .

24 msec after the end of the previous measurement. The peak-to-peak temperature variation in figure 10 is  $11\ 000^\circ\text{K}$  and the standard deviation, defined in the usual manner, is  $2300^\circ\text{K}$ , or about 10 percent of the mean  $T_e$  value. Consequently, the time and space fluctuations in data such as those presented in figure 9(a) can to some extent be separated by fairing a curve through the data points, but the resolution will be limited by the standard deviation for electron temperatures at the same conditions. Such an averaging procedure has been carried out in figure 9(b), where the dashed lines correspond to  $\pm\sigma$  as obtained from figure 10. Figure 9(b) indicates the way in which  $T_e$  distributions must

be presented: The electron temperature at each point in space is given as an average value with upper and lower limits based on the standard deviation of time fluctuations at the same operating conditions. The average value may be determined either by fairing a curve through the data as in figure 9(b) or by using the results of a plot such as figure 10, repeated for several radial positions. Note the agreement between the two mean  $T_e$  values for the example of figures 9 and 10: The computed mean value of figure 10 is  $26\ 500^\circ\text{K}$ , while figure 9(b) has an apparent mean value of about  $27\ 000^\circ\text{K}$  at  $r = 0$ .

It is apparent that the existence of an erratic low-frequency  $T_e$  fluctuation as previously described (i.e., roughly constant for 8 msec but different 24 msec later) will sometimes produce  $\ln I_e$ - $V$  curves which appear non-Maxwellian if a rather abrupt change in some plasma parameter occurs during the 2 msec required to sweep the electron-current part of the probe curve (see fig. 7). Such a curve is shown in figure 11. If data such as these are obtained regularly – that is, if the fluctuation frequencies more nearly correspond to the time required to record the electron current – the present system cannot be used without modification. Ideally, the modification would consist of a faster probe sweep so that  $T_e$  would again appear constant during the course of a measurement for most of the probe curves obtained.

The question of interpreting Langmuir probe curves becomes more complex when the effect of high-frequency noise is considered. Since the frequency spectrum of the curves in this study is limited by filtering to less than 2000 Hz, higher discrete frequencies are eliminated. Nonetheless, the coherent oscillations in the 10 kHz range typical of MPD arc devices (and observed in the present device) can manifest themselves as apparently random scatter in the data, especially when the voltage level of such oscillations is a sizable fraction of the total arc voltage. In addition, there is an abundance of possible arc noise sources in the range of 100 to 2000 Hz. Sometimes these may appear coherent, as in the case of power-supply ripple. Otherwise, the noise is apparently random, arising from incompletely understood electrode or ionization phenomena.

On probe traces, the source of any noise is, of course, unidentified; it merely produces voltage or current fluctuations on the  $I$ - $V$  characteristic. A simultaneous high-frequency variation in plasma potential, local density, and electron temperature would seemingly be the most probable situation. (Bear in mind that the  $T_e$  fluctuations under consideration now would have a frequency much higher than  $\frac{1}{2\ \text{msec}} = 500\ \text{Hz}$ .) However, it has been shown by Sugawara and Hatta (ref. 6) that even small high-frequency  $T_e$  fluctuations result in a distortion of the linearity of the  $\ln I_e$ - $V$  curve. This distortion is prominent around the floating potential, that is, in the high-energy tail of the electrons. Therefore if, as with the large majority of curves obtained in the hollow-cathode device, the scatter on curves seems to fall naturally about a straight, rather than a curved, line, it can be concluded that the scatter on probe curves is not due to high-frequency  $T_e$  fluctuations. Potential and density fluctuations do not significantly affect the value of

$T_e$  even when the scatter is large, as demonstrated by Chen (ref. 7), and hence the temperature obtained from noisy curves is still a meaningful result.

This conclusion adds another qualitative aspect of data reduction which reemphasizes the necessity for visual inspection of all results as previously described. First, it is necessary to decide when the peak-to-peak voltage fluctuations on a particular curve

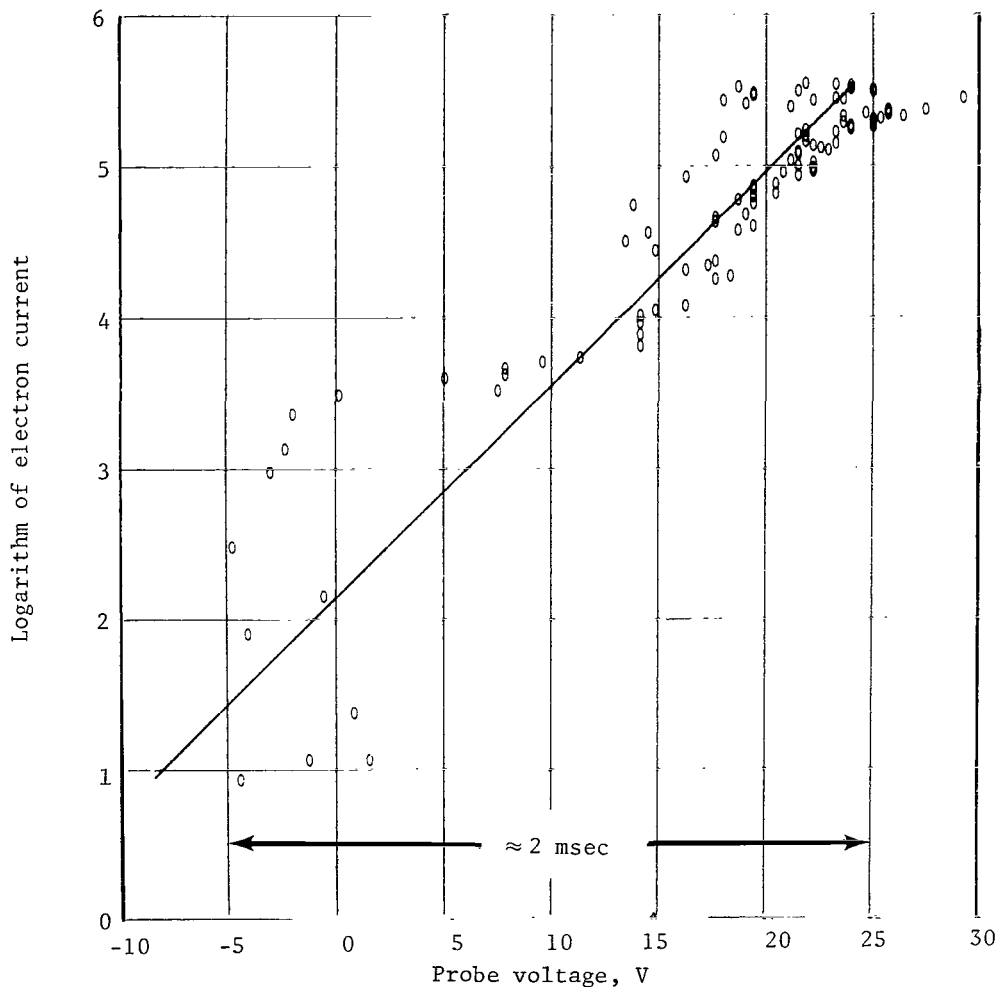
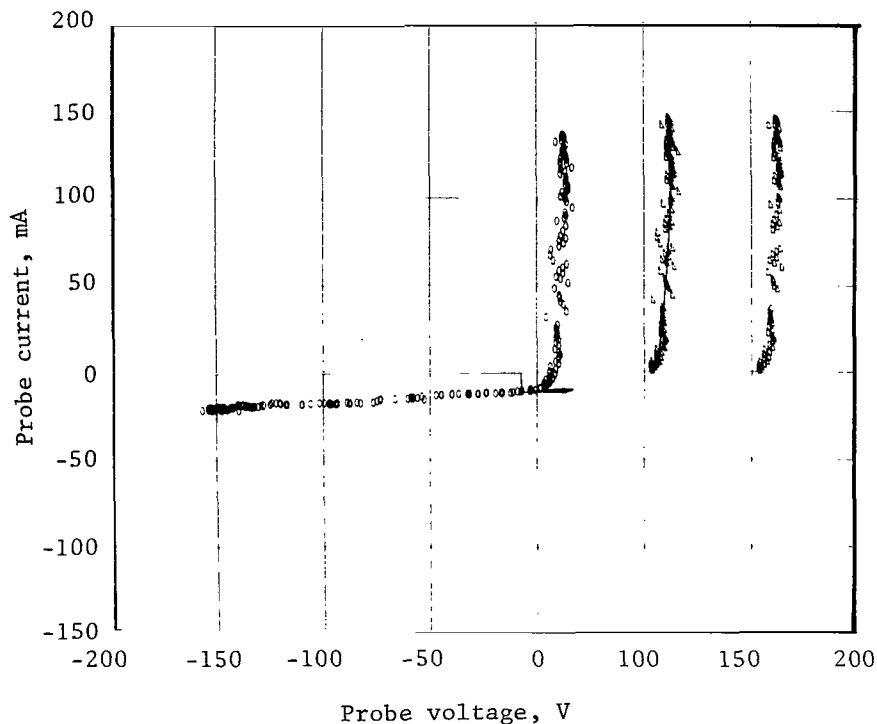
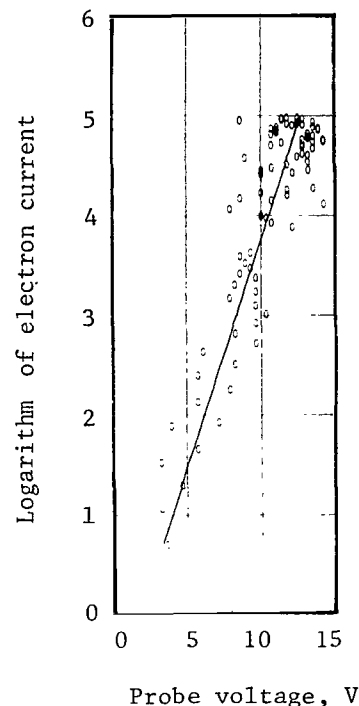


Figure 11.-  $\ln I_e$ - $V$  plot showing the effect of a large fluctuation at about 1 kHz.

are so large that the resulting temperature is questionable. Certainly, a curve for which the peak-to-peak voltage fluctuation at a particular current is much larger than the voltage equivalent of the calculated temperature would be suspect ( $1 \text{ eV} = 11\,600^\circ \text{K}$ ), although it is felt that the  $\ln I_e$ - $V$  plot of figure 12, for example, still yields a useful result. Second, a reasonable question would be whether or not it is possible to base a positive mathematical criterion for acceptability on the standard deviation of points about the line fitted to the  $\ln I_e$ - $V$  data points, and thereby eliminate a considerable amount of labor.



(a) I-V plot.



(b)  $\ln I_e$ -V plot.  
 $T_e = 25\ 200^{\circ}\text{ K}$ .

Figure 12.- I-V and  $\ln I_e$ -V plots showing the effect of potential fluctuations on electron current.

Unfortunately, this would be difficult, for a  $\ln I_e$ -V curve with small scatter might be obviously bowed, while a curve with considerable scatter might yield a reasonable straight-line fit.

In the present studies, a flexible attitude has been adopted with regard to the credibility of the temperature associated with a particular curve for the following reason: The standard deviation associated with the electron temperature assigned to a particular point in space, being on the order of 5000 to 10 000<sup>o</sup> K, may be considered large with respect to the error introduced by accepting a particular calculated value. For example, if, as in figure 10, a time-averaged temperature value must be given as  $T_e$  plus or minus approximately 10 percent, it is not unreasonable to accept a particular temperature value such as that for the noisy data of figure 12, which by all available evidence is correct within a few percent.

## CONCLUSIONS

1. FM tape recording and digital-computer techniques can be combined to provide an automated data reduction system for large quantities of Langmuir probe data obtained in a high-power magnetoplasma dynamic arc.

2. Electron-temperature distributions can be obtained over a wide range of operating conditions by using computer techniques that take into account extreme variations in the detailed behavior of the probe data.

3. Because of the random nature and time scale of electron-temperature fluctuations, scatter in spatial surveys can be averaged when data are taken in the manner described. The surveys then consist of averaged curves based on the shape of the data, with an error bar based on the standard deviation for temperature values obtained at the same operating conditions and location as a function of time.

Langley Research Center,  
National Aeronautics and Space Administration,  
Langley Station, Hampton, Va., June 7, 1967,  
129-01-05-04-23.

#### REFERENCES

1. Eggers, G. H.; and Schwirzke, F.: A Method of Using a Computer To Evaluate Langmuir Probe Data for Obtaining the Electron Temperature. Proceedings of the 1965 Symposium on Engineering Problems of Controlled Thermonuclear Research, Contract W-7405-ENG-48, Lawrence Radiation Lab., Univ. of California, May 1965, pp. 96-99.
2. Chen, Francis F.: Electric Probes. Plasma Diagnostic Techniques, Richard H. Huddlestone and Stanley L. Leonard, eds., Academic Press, 1965, pp. 113-200.
3. Weinstein, Richard H.; and Hoell, James M.: Experiments in a Hollow Cathode Hall Current Accelerator. AIAA Paper No. 65-299, July 1965.
4. Sugawara, Minoru: Electron Probe Current in a Magnetized Plasma. Phys. Fluids, vol. 9, no. 4, Apr. 1966, pp. 797-800.
5. Sonin, Ain A.: Free-Molecule Langmuir Probe and Its Use in Flowfield Studies. AIAA J., vol. 4, no. 9, Sept. 1966, pp. 1588-1596.
6. Sugawara, Minoru; and Hatta, Yoshisuke: Langmuir Probe Method for a Plasma Having Small Amplitude Oscillations. Res. Rept. IPPJ-4, Nagoya Univ., Feb. 1963.
7. Chen, Francis F.: Double-Probe Method for Unstable Plasmas. Rev. Sci. Instr., vol. 35, no. 9, Sept. 1964, pp. 1208-1212.



*"The aeronautical and space activities of the United States shall be conducted so as to contribute . . . to the expansion of human knowledge of phenomena in the atmosphere and space. The Administration shall provide for the widest practicable and appropriate dissemination of information concerning its activities and the results thereof."*

—NATIONAL AERONAUTICS AND SPACE ACT OF 1958

## NASA SCIENTIFIC AND TECHNICAL PUBLICATIONS

**TECHNICAL REPORTS:** Scientific and technical information considered important, complete, and a lasting contribution to existing knowledge.

**TECHNICAL NOTES:** Information less broad in scope but nevertheless of importance as a contribution to existing knowledge.

**TECHNICAL MEMORANDUMS:** Information receiving limited distribution because of preliminary data, security classification, or other reasons.

**CONTRACTOR REPORTS:** Scientific and technical information generated under a NASA contract or grant and considered an important contribution to existing knowledge.

**TECHNICAL TRANSLATIONS:** Information published in a foreign language considered to merit NASA distribution in English.

**SPECIAL PUBLICATIONS:** Information derived from or of value to NASA activities. Publications include conference proceedings, monographs, data compilations, handbooks, sourcebooks, and special bibliographies.

**TECHNOLOGY UTILIZATION PUBLICATIONS:** Information on technology used by NASA that may be of particular interest in commercial and other non-aerospace applications. Publications include Tech Briefs, Technology Utilization Reports and Notes, and Technology Surveys.

*Details on the availability of these publications may be obtained from:*

SCIENTIFIC AND TECHNICAL INFORMATION DIVISION  
NATIONAL AERONAUTICS AND SPACE ADMINISTRATION

Washington, D.C. 20546